

# Methodology for a Numerical Analysis of the Aerodynamic Performance of a Centrifugal Fan Trough Computational Fluid Dynamics (CFD)

**Darwin Omar Maestre Di Cioccio**  
**Ramiro Gustavo Ramirez Camacho**  
**Waldir de Oliveira**  
**Tania Marie Arispe Angulo**

Federal University of Itajubá - UNIFEI, BPS. Av, 1303, Bairro Pinheirinho, Itajubá, MG - Brazil  
Institute of Mechanical Engineering - IEM  
Virtual Hydrodynamics Laboratory - LHV  
darwin.maestre@unifei.edu.br  
ramirez@unifei.edu.br  
waldir@unifei.edu.br  
tani.arispe86@gmail.com

**Abstract.** Centrifugal fan and compressors are widely utilized in engineering practices. A numerical investigation of the backward-curved blades centrifugal fan performances is presented in this work. The experiments were produced in another work in order to get the performances in different flow conditions to the specific impeller. The internal flow field in the impeller was calculated by means of Computational Fluid Dynamics techniques. Numerical and experimental results are compared together for a large range of flow rate. Furthermore, simulations were performed in the steady regime. Several analyses of the numerical results are presented and some comments are made on the validity of the application of CFD techniques is appropriate to obtain the aerodynamic behaviour characteristics of this type of turbomachine.

**Keywords:** CFD, Centrifugal Impeller, Turbomachinery, Aerodynamic Performance Characteristics.

## 1. INTRODUCTION

Centrifugal fans are used for their ability to generate a relatively high total pressure rise at a reasonable compact size and are a common type of turbomachinery that are widely used in the ventilation systems of ships cabins and other sites, and they help provide comfortable working and living environments for people. It is found that a numerical approach using a design analysis tool like CFD is of recent origin and the whole field flow analysis of the complex flow in a centrifugal fan has been the state of the art in the domain. Many studies have examined three-dimensional complex flow fields to improve the aerodynamic performance of backward-curved blade centrifugal fans using a range of experimental and computational methods.

Although aerodynamic performance has historically been scaled from previous laboratory test data, the impeller, shaft and housing mechanical design, bearing selection and rotor-dynamic analysis are invariably unique.

The agreement between the numerical results and test data is also difficult because the numerical result is very sensitive to the numerical method, including mesh generation, boundary condition handling, turbulent model selecting, and data processing. Zhang *et al.* (1996) computed the three-dimensional viscous flow in a blade passage of a backswept centrifugal impeller at the design point with the standard  $k-\epsilon$  model. The comparison of computed and measured values showed good agreement.

Through numerical simulation, Liu *et al.* (2008) analyzed the three-dimensional flow field of a centrifugal fan, carried out a numerical study on the inner flow field of a multi-blade centrifugal fan using Reynolds-averaged Navier-Stokes equations and RNG  $k-\epsilon$  turbulence model. Some important flow phenomena were predicted. Combined with experimental studies, effects of the blade inlet angle and the impeller tip clearance on the flow efficiency were investigated. These are useful for the optimum design of the multi-blade centrifugal fan.

With the rise development of calculation methods and computer techniques, the complete three - dimensional numerical method is applied to the inner flow simulation of a centrifugal fan. Research efforts have been made to simulate complicated three - dimensional viscous flows by using different numerical methods and to study unstable flows Haifeng *et al.* (2001); Seo *et al.* (2003); Chunxi *et al.* (2011); Darvish (2015); Kim *et al.* (2012); Yu *et al.* (2005); Liu, Jiawei (2012); The results obtained improved greatly the design of impeller machines.

In this paper, the flow in an impeller passage is simulated using a  $k-\omega$  SST turbulence model. According to Galarça (2004), this model can solve the problems of the models  $k-\omega$  and  $k-\epsilon$ , i.e, in sections with curvatures and near to the wall, is used the model  $k-\omega$ , and in sections far of the wall is used the model  $k-\epsilon$ . The model SST is used as the turbulence closure and provides accurate predictions for flow cases with adverse pressure gradients involving separation, Menter (1993).

In the present work we chose two commercial software for geometry creation, computational mesh generation, boundary condition definitions and post processing are performed through ICEM-CFD®17.2 and FLUENT®17.2 respectively.

## 2. REFERENCE CENTRIFUGAL FAN

### 2.1 Physical model

In general, a centrifugal fan is composed of an inlet nozzle, a radial or approximately radial impeller and a scroll. Figure 1 shows a typical centrifugal rotor scheme with the meridian and transversal section of the impeller with a simple backward curved blades  $\beta_5 < 90^\circ$ , where the blades are integral with the internal disc mounted on the fan shaft and the external disc (hub). The blades are usually fixed perpendicular to these discs. Such a configuration is called a closed impeller, typical of centrifugal fans.

The fan impeller consists of 10 backward curved shape blades in the arc format, the volume flow rate at design point is  $0,35 \text{ m}^3/\text{s}$ . The impeller width at the inlet  $b_4 = 71,141 \text{ mm}$ . The additional design specifications in the current analysis are listed in Table 1.

Table 1. Dimensional specifications for the centrifugal fan

Rotational frequency of impeller, rps	314,16
Outlet diameter of impeller, mm	419,5
Inlet diameter of impeller, mm	207,6
Blade thickness, mm	3,0
Inlet set angle, ( $^\circ$ ) $\beta_4$	31,87
Outlet set angle, ( $^\circ$ ) $\beta_5$	50,41
Impeller width $b_5$ , mm	32,1
Number of main blades	10

The impeller inlet and outlet velocity diagrams are located at points 4 and 5 respectively, validation of the numerical results is performed through experimental data of de Oliveira (2001). The impeller has a specific rotation of  $n_{qA} = 150$ , defined by

$$n_{qA} = 10^3 \frac{nQ^{1/2}}{Y^{3/4}} \quad (1)$$

where  $n$  is the rotational speed of the rotor in rps,  $Q$  is the volumetric flow in  $\text{m}^3/\text{s}$ , and  $Y$  represents the specific work of the turbomachine in  $\text{J}/\text{kg}$ .

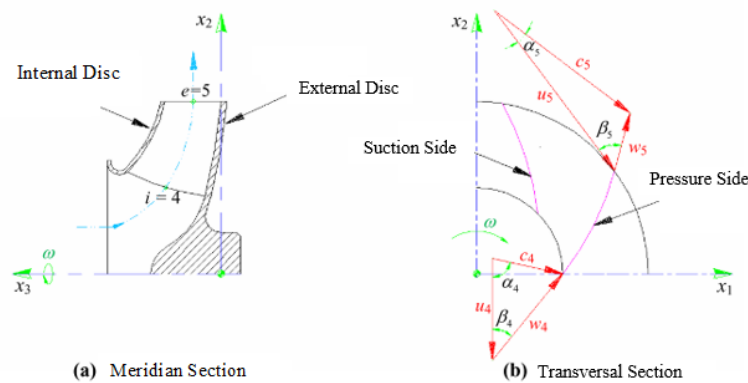


Figure 1. Centrifugal fan scheme and velocity triangles to inlet and outlet of impeller.  
 Available from: Gamboa (2013)

### 2.2 Global characteristics

According to experimental test, the flow and total pressure rise coefficients at the design flow condition of the reference model are 0.323 and 1.147, respectively, with an hydraulic efficiency of 94.9%, which are defined as,

$$\psi = \frac{2Y}{\rho u_5^2} \quad (2)$$

$$\phi = \frac{Q}{AU_t} \quad (3)$$

where,  $Q$ ,  $\Delta_{pT}$ ,  $U_5$ , and  $\rho$  indicate the volume flow rate, total pressure rise, rotor tip speed, and density, respectively, and  $A$  is the outlet area of a centrifugal fan.

Centrifugal impellers are normally operated in volute casings, most often without outlet guide vanes with the casing spiral being the only means to guide the flow and to convert kinetic flow energy to potential energy (increased static pressure). In this work centrifugal fan impeller is solved without volute casing irregular external interference. Only the impeller are chosen and these calculation results are compared with experimental ones.

The individually analysis of each component, according to Jakipse and Platt (2004), is done with the objective to reach the best possible performance for a given turbomachine application. The isolated treatment of each component is a remarkable simplification, but the problems related to the actual flow persist, particularly when it comes to a centrifugal rotor, due to its rotation and geometry.

Therefore, further simplifications should occur, however, preserving as much as possible the actual flow characteristics in each compliant component according to Violato (2004).

### 3. NUMERICAL METHODOLOGY

A three-dimensional numerical simulation of the complete steady flow in the centrifugal impeller is carried out. Calculations are performed with a commercial software package, FLUENT®17.2. This code uses the finite volume method and the three-dimensional Navier–Stokes equations are solved on an structured and unstructured grid system.

Among the steps of numerical methodology to be applied in this work for the analysis and aerodynamics prediction of centrifugal fan, will apply the principles of conservation of mass and the quantity of motion.

#### 3.1 Geometry of the centrifugal impeller

A geometrical discretization for the numerical treatment of the centrifugal impeller is generated by using ANSYS ICEM®CFD 17.2. A view of the impeller geometry can be seen in Figure 2.

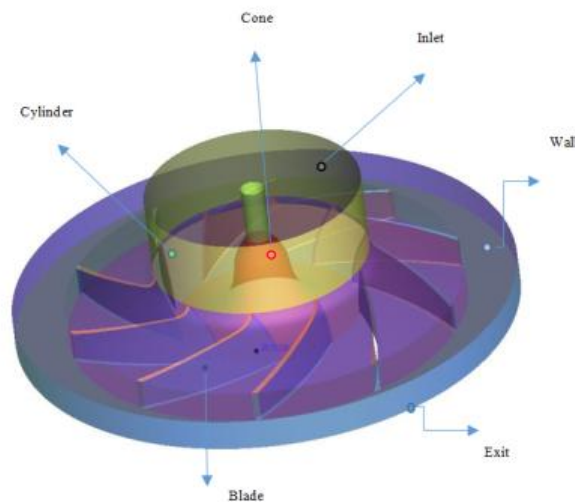


Figure 2. Computational domain of the centrifugal impeller

The three dimensional flow domain of the centrifugal fan is same in geometry size as the fan in the experiment. This computational domain includes a rotating impeller domain and three stationary domains (casing disc, inlet, and exit domains).

#### 3.2 Mathematical model

Numerical modeling is divided into the discretization step of the flow domain and numerical simulation of the centrifugal fan. The commercial software FLUENT®17.2 was used to simulate the centrifugal impeller. This solves the Navier-Stokes equation using the finite volume method (FVM), which has been applied widely in fluid mechanics and engineering applications.

The computations, which include mesh generation, simulation and post-processing, have been performed by an cluster with Intel-Xeon processor having clock speed of 2.6 GHz, 32 core and 128 GB of RAM. The converged solutions were obtained after 1200 iterations and the computational time was about approximately 6 hrs.

This work also aims to estimate a wide range of fan operation to determine hydraulic performance values based on computational studies.

All points of operation of the fan was studied in situations of permanent regime according to Liu *et al.* (2008) by means of turbulence models based on the analyses of the Reynolds tensors.

The Reynolds-averaged  $k-\omega$  SST turbulence model is used, which is a compounded model of the  $k-\omega$  model and the  $k-\epsilon$  model, so it is reliable in calculating the near-wall viscous flow as the  $k-\omega$  model and accurate in calculating far-field free flow as the  $k-\epsilon$  model. It was demonstrated that the SST model captures flow separation under adverse pressure gradient well compared to other eddy viscous models and predicts well the near wall turbulence which is vital for the accurate prediction of flow separation.

#### 4. COMPUTATIONAL DOMAIN

This section states grid system generation, boundary condition settings and numerical solution control of this study. The computational domain is divided into two zones, a rotational zone including the impeller and stationary zones else where. The CAD of this configuration, as well as the boundary conditions, was shown in Figure 2.

##### 4.1 Mesh generation

In the pre-processing stage of the simulation the analysis and capture of the physical phenomena of turbulent flow depends on the treatment of wall shear stress. To ensure the accuracy of numerical analysis and the calculation of the different variables of interest in the flow, it is necessary to determine the appropriate size of the mesh elements by the dimensionless parameter  $y^+$ , defined as the size of the first layer from the wall to the first node. The  $y^+$  parameter can be obtained from the Equation 4, where  $\mu$  is the dynamic viscosity of the fluid.

$$y^+ = \frac{\rho y u_r}{\mu} \quad (4)$$

To improve the calculation accuracy, the size function is used to encrypt the mesh in some key regions such as the blade edges, the value of the parameter  $y^+$  adopted in this work was 25 and the value for the distance from the wall to the first element was  $(0.4 \times 10^{-4} \text{ m})$ , calculated in order to accurately capture the shear stress on the wall and implement a low Reynolds for the SST numerical model.

##### 4.2 Mesh independence test

The mesh independence studies were carried out before results and final analysis by three different meshes numbers of 7,886,461, 11,119,161 and 17,756,071. The impeller has 11,119,161 nodes and 10,826,300 elements with maximum size of the element is limited to having an edge length of 0.04 mm. However to establish grid independence, analysis were carried out with large element size meshed models having element edge lengths of 1.5 mm and 1 mm.

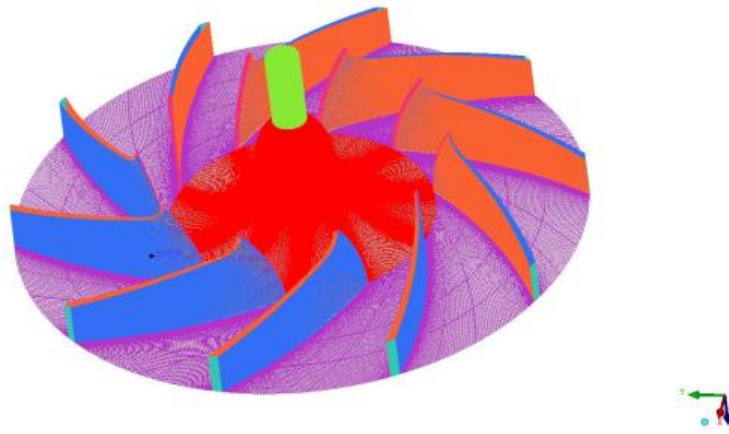


Figure 3. Mesh distributions of the computational domain

The appropriately sized grids were chosen to make sure grid will not impact the studies, i.e., the analyses are not grid dependent. The meshed model of baseline fan is shown in Figure 3 with refinement near to the leading and trailing edge to ensure reliable results of power shaft and hydraulic efficiency.

##### 4.3 Boundary Conditions

In CFD one of the major difficulties is the determination of the accuracy of the solution and definition of boundary conditions. Surfaces that rotate relatively are defined as “moving wall”. Moreover, as they are dependent on the fluid

around them and as they rotate, they are defined as “relative to adjacent cell zone” and “rotational motion”. Cylinder walls are defined as “stationary wall” and the inlet and outlet are defined as “velocity inlet” and “pressure outlet”. Fluid zone in the inner volume is defined as “rotational” and a constant angular velocity of 314.16 rad/s in Z-direction, this assumes that the inlet velocity is uniform in each grid node and the flow direction is perpendicular to the nozzle inlet surface. The turbulence intensity is assumed to be 5% and furthermore, the turbulent viscosity ratio is assumed to be five. At outlet of the computational domain, the static pressure is assumed to be the standard atmosphere and the backflow turbulence intensity is 10% and the backflow turbulent viscosity ratio is ten. All of the wall boundary conditions in the impeller are regarded as no-slip conditions. The working fluid was considered to be an ideal gas with the specific mass and the dynamic viscosity of  $\rho= 1,225 \text{ kg/m}^3$  and  $\mu= 1,7894 \times 10^{-5} \text{ kg/m}$  respectively.

#### 4.4 Assumptions and numerical model

In this study, several assumptions were made to facilitate the simulations: incompressible flow, no-slip boundary condition, gravity effects are negligible and fluid properties are not functions of temperature.

Three different numerical solution schemes were employed, for the coupling between the pressure and velocity fields the SIMPLE algorithm was used with primary order upwind difference interpolation, necessary for a run to converge down to Root-mean-square (RMS) values of the equation residuals for convergence criteria were specified to be at least ( $\epsilon=10^{-4}$ ) for all equations according to the values recommended by ANSYS (2017) for academic research.

In the pressure interpolation the *standard* scheme was used, in this scheme the values of the pressure on the cell faces are interpolated using coefficients of the momentum equation. For the numerical solution of the equations of momentum, turbulent kinetic energy and specific dissipation rate, the first order precision upstream scheme is used because achieve better convergence than second-order scheme ANSYS (2017). Table 2 shows the solution methods adopted for steady state simulations.

Table 2. Scheme solutions

Time	Solution Methods
	Pressure Velocity - Coupling Scheme: SIMPLE
<b>Steady</b>	Spacial Discretization: Gradient: Least Squares Cell Based Pressure: Standard Momentum: First Order Upwind Turbulent Kinet Energy: First Order Upwind Specific Dissipation Rate: First Order

The simulations shows an unstable behavior in each iteration in the solution of the set of equations to be solved, the standard FLUENT®17.2 sub-relaxation factors were changed, considering the convergence and the stability of the residual curves during calculations. Table 3 presents the values of the relaxation factors used.

Table 3. Relaxation factors

Variable	Relaxation Factors
Pressure	0,3
Density	1,0
Body Forces	1,0
Momentum	0,4
Turbulent Kinetic Energy	0,7
Specific Dissipation Rate	0,7
Turbulent Viscosity	1,0

## 5. RESULTS AND DISCUSSIONS

### 5.1 Impeller performance curves analysis

The overall performance of this centrifugal impeller predicted by the CFD calculations and was compared with the experimental results obtained from de Oliveira (2001) for different flow conditions.

The best efficiency point  $\eta = 94,822$  at a rotational speed  $\pm 3000$  rpm corresponded to a volume flow rate  $Q = 0,8641$   $kg/s$ , flow rate coefficient of ( $\phi = 0.3099$ ), and a total pressure rise  $\Delta_{pT} = 3019$  Pa, and a pressure coefficient of ( $\psi = 1.0791$ ). The hydraulic efficiency, the pressure differential, the hydraulic power and shaft power dependencies are provided in Figure 4.

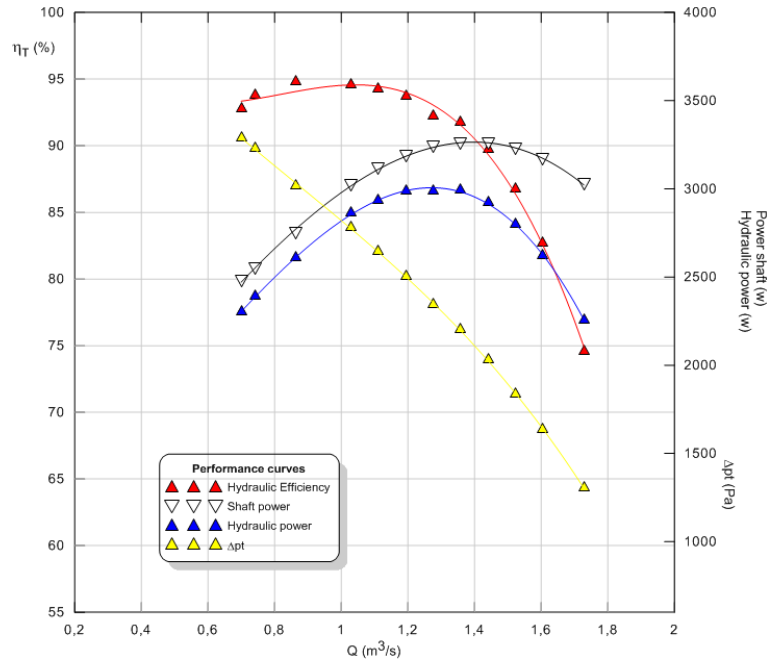


Figure 4. Performance curves of the centrifugal fan obtained by numerical simulations.

For the validation of the present numerical solutions, the characteristics of a hydraulic efficiency of the reference impeller were compared to the experimental results according to the flow rate coefficient, as shown in Figure 5, where the characteristics of the flow coefficient and efficiency obtained by numerical simulation match well with the experimental results.

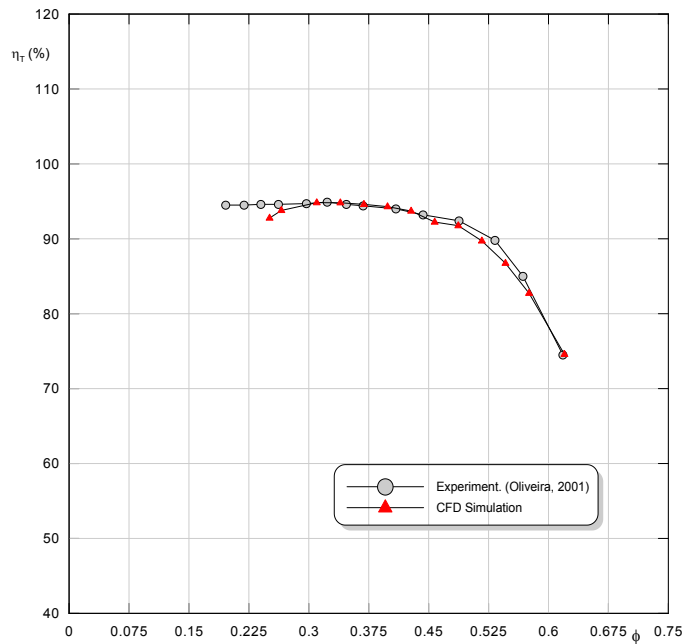


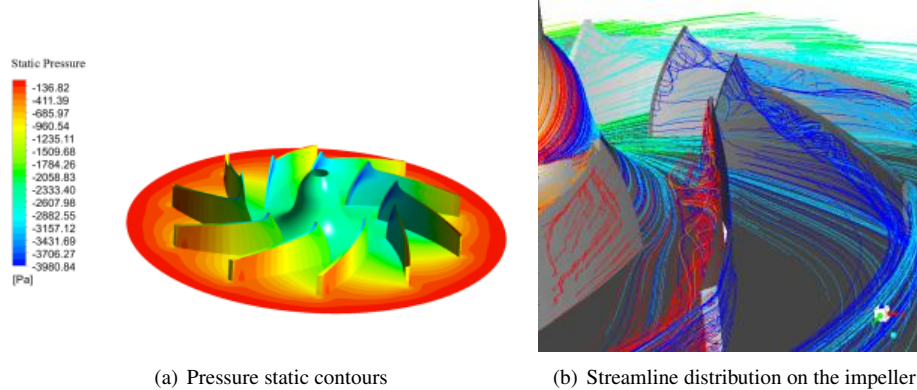
Figure 5. Validation of the numerical analysis

The comparisons between the numerical and experimental results near the design flow condition show that the pressure and efficiency of the test fan are simulated correctly. Thus, it is assured that the numerical analysis is valid and reliable.

## 5.2 Analysis on flow characteristics of impeller

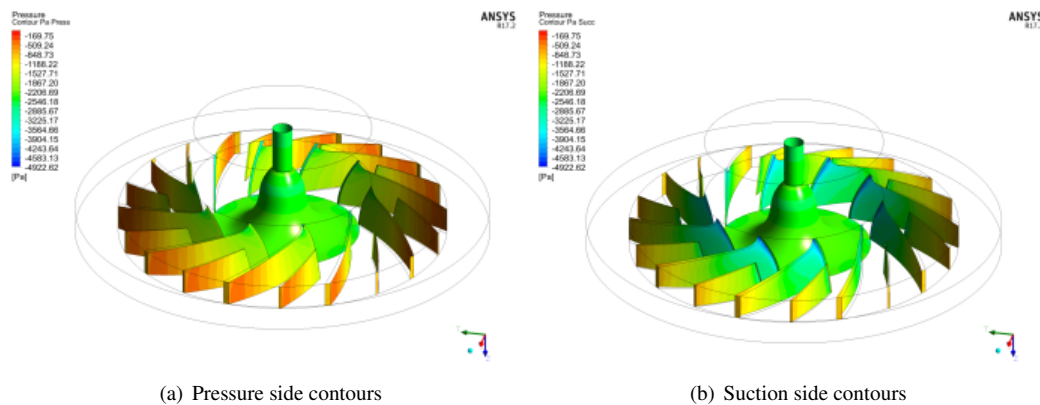
Flow analysis and post processing are performed through CFD-Post 18.2 and FLUENT®17.2, respectively. Figure 7(a) and 7(b) give comparison of the instantaneous static pressure distribution pressure and an instantaneous picture of the streamlines of the impeller inlet. It can be seen that pressure drop of the impeller appeared in the leading edge suction side of blade passage, thus, it will affect the total pressure flow. The blades and the friction of the rotating hub gradually impose a pre-swirl on the inflow and cause the formation of an inlet vortex which indicates flow loss, and result in negative pressures.

Figure 6. Comparison of the pressure contours of the impeller with streamline distribution



From Figure 7(b), it is clear seen that low pressure load means at suction side and high pressure at pressure side. However an obvious pressure increase and relative velocity decrease were observed near the trailing edge in the impeller at 50% spanwise position Figure 7(a).

Figure 7. Pressure contours of the impeller



## 6. ACKNOWLEDGEMENTS

The authors thank the Postgraduate Mechanical Engineer Program of Federal University of Itajubá. The (LHV) Laboratory of Virtual Hydrodynamic and the Coordination for the Improvement of University Education Personnel (CAPES), for financial support.

## 7. CONCLUSIONS

Both numerical simulation and experiment test has been performed to analyze the aerodynamic performance of a backward blades centrifugal fan. We concluded that the overall CFD predictions are satisfactory to predict the aerodynamic performance curves match quite well with the experimental ones, indicating that, the steady flow simulations could be used. From results of the flow analysis, considerable energy loss by flow separation was observed in the blade passages. The performance of the centrifugal fan decreases and the efficiency drops by about 1–2% because of the flow loss in the blade passage.

## 8. REFERENCES

- ANSYS, 2017. *FLUENT Theory Guide*. Academic Research Mechanical.
- Chunxi, L., Ling, W.S. and Yakui, J., 2011. "The performance of a centrifugal fan with enlarged impeller". *Energy Conversion and Management*, Vol. 52, No. 8-9, pp. 2902–2910.
- Darvish, M., 2015. *Numerical and experimental investigations of the noise and performance characteristics of a radial fan with forward-curved blades*. Ph.D. thesis, Universität Berlin.
- de Oliveira, W., 2001. *Análise do Escoamento em Turbomáquinas radiais*. Ph.D. thesis, Instituto Tecnológico de Aeronáutica, São José dos Campos, Brasil.
- Galarça, M.M., 2004. "Análise Numérica Para Modelos De Turbulência  $k-\omega$  e  $k-\omega$  SST para o Escoamento de Ar no Interior de uma Lareira de Pequeno Porte".
- Gamboa, Y.F.Q., 2013. *Análise da Interação Rotor-Voluta de Turbomáquinas Centrífugas por Meio do Escoamento Potencial Levando em Consideração a Variação da Geometria e Espaçamento das Pás do Rotor*. Master's thesis, Universidade Federal de Itajubá.
- Haifeng, L., Yulin, W. and Zhimei, Z., 2001. "The determination of centrifugal pump impeller's design with three-dimensional turbulent flow simulation". *Fluid Machinery*, Vol. 9.
- Jakipse, D. and Platt, M.J., 2004. "Optimization in component design and redesign". In *The 10th International Symposium on Transport Phenomena and Dynamics of Rotating Machinery*.
- Kim, J.H., Cha, K.H., Kim, K.Y. and Jang, C.M., 2012. "Numerical investigation on aerodynamic performance of a centrifugal fan with splitter blades". *International Journal of Fluid Machinery and Systems*, Vol. 5, No. 4, pp. 168–173.
- Liu, X., Dang, Q. and Xi, G., 2008. "Performance improvement of centrifugal fan by using cfd". *Engineering Applications of Computational Fluid Mechanics*, Vol. 2, No. 2, pp. 130–140.
- Liu, Jiawei, 2012. *Simulation of whistle noise using computational fluid dynamics and acoustic finite element simulation*. Master's thesis.
- Menter, F., 1993. "Zonal two equation kw turbulence models for aerodynamic flows". In *23rd fluid dynamics, plasmadynamics, and lasers conference*. p. 2906.
- Seo, S., Kim, K. and Kang, S., 2003. "Calculations of three-dimensional viscous flow in a multiblade centrifugal fan by modelling blade forces". *Proceedings of the Institution of Mechanical Engineers, Part A: Journal of Power and Energy*, Vol. 217, No. 3, pp. 287–297.
- Violato, M.O., 2004. *Análise Teórica do Escoamento em Rotores Centrífugos com Pás Auxiliares*. Master's thesis, Universidade Federal de Itajubá.
- Yu, Z., Li, S., He, W., Wang, W., Huang, D. and Zhu, Z., 2005. "Numerical simulation of flow field for a whole centrifugal fan and analysis of the effects of blade inlet angle and impeller gap". *HVAC&R Research*, Vol. 11, No. 2, pp. 263–283.
- Zhang, M.J., Pomfret, M. and Wong, C., 1996. "Three-dimensional viscous flow simulation in a backswept centrifugal impeller at the design point". *Computers & fluids*, Vol. 25, No. 5, pp. 497–507.